

**ПОДХОДИ ЗА БЪРЗ ЗАРЯД НА БАТЕРИИ ЗА ЕЛЕКТРОМОБИЛИ**  
**APPROACHES FOR FAST CHARGING OF ELECTRIC VEHICLE BATTERIES**

**Stoyan Vuchev**  
Technical University of Sofia, Bulgaria

**Dimitar Arnaudov**  
Technical University of Sofia, Bulgaria

**Abstract**

The following paperwork presents results from research of different approaches for charging of electric vehicle batteries. Latest tendencies and general problems with the plug-in electric vehicles are overviewed, main battery parameters and options for battery charging are discussed. Standards for fast charging are considered. Approaches for fast DC charging based on modular system realization are proposed. Simulation examinations for verification of the proposed system topologies are carried out. Basic dependencies of the investigated modular converters are obtained.

**Keywords:** Electric Vehicles, Fast Charging, Modular Systems, Resonant Converters.

**INTRODUCTION**

Electric vehicles (EVs) become more and more popular nowadays due to the decrease in the battery prices. Moreover, governments and local authorities offer different grants and preferences for buying an EV.

Fig. 1 presents the global sales of plug-in electric vehicles (PEV) in the recent years [1]. It can be seen that nowadays the PEV market share is only about 1% but it quickly rises. According to a recent research [2], by 2040 this share is expected to reach about 35% of all new vehicle sales (fig. 2) due to the expectations that by 2022 EVs will cost the same as their internal-combustion counterparts.

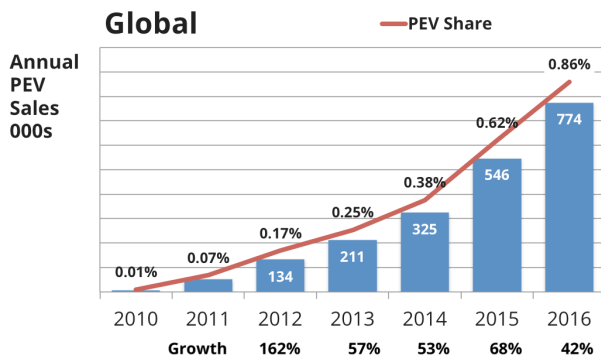


**Fig. 1.** Global PEV sales and PEV share in the recent years [1].

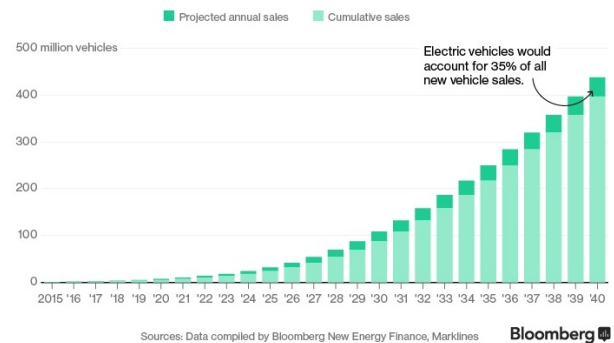


**Fig. 2.** EV sales projections by 2040 [2].

Still, a major drawback is the limited travel range due to the small battery capacity in most of the modern EVs, which makes them more suitable for short-distance transportation. A possible solution to this problem is the fast charging option allowed by the lithium battery technology [3, 4]. However, fast charging requires significant currents to be applied, which is a challenge to the power electronic converters. High efficiency, galvanic isolation and proper grid parameters are often necessary.

The following paperwork considers modular DC-DC converters for fast charging of EV batteries. Topologies with parallel and series load connection of the modules are investigated. Results from computer simulations are used for verification and comparison between the examined circuits.

## PEV BATTERIES AND CHARGING STATIONS

Table 1 presents main battery parameters of some of the most common EVs [5]. It also provides information for the cars estimated driving range with respect either to the United States *Environmental Protection Agency (EPA)* standards or to the *New European Driving Cycle (NEDC)* standard. Additional data about the different opportunities for charging and the estimated complete charge times are presented as well (specificities and limitations are presented in italics).

From Table 1, it can be seen that the average estimated EV driving range (excluding Tesla cars as an exception) is about 150 km compared to the average 800-1000 km driving range of the internal-combustion cars. Due to road and traffic specificities, the real driving range is usually shorter, and driving with higher speed additionally shortens it.

Using an AC charger for home applications, the average time for complete battery charge is about 6-7 hours with 3.6kW (~230V/16A) or 4-5 hours with 7kW (~230V/32A) power. Higher power is not usually applied for domestic uses, and some of the EVs do not implement more powerful on-board AC chargers.

Thus, in order to significantly reduce the complete charge time, fast charging methods are necessary. Most of the modern EVs support fast charging according to one or more standards the most common of which are as follows:

- **IEC 62196 Type 2** – commonly referred to as *Mennekes* after the name of the company proposing it. It is originally specified for EV charging at 3 ÷ 120kW single-phase AC, three-phase AC or DC [6]. The most common fast AC chargers implement 43kW power at three-phase 63A supply. The DC charging option after a slight connector modification is known as *CCS*.
- **CCS** – an abbreviation of “Combined Charging System”, also known as *Combo2* [7]. This DC charging standard enables EV charging with up to 150kW. The most common car chargers implement 50kW power at nominal current about 120A.
- **CHAdemo** – an abbreviation of “CHARGE de MOve”. This is a DC charging protocol currently enabling EV charging with power from 6 to 200kW via a special connector [8, 9]. The most

EV Model	Battery Capacity [kWh]	Nominal Battery Voltage [V]	Range [km]	Complete Charge Time [h]					
				~230V 3.6kW	~230V 7kW	~400V 43kW	CHAdemo DC 20-50kW	CCS DC 20-50kW	TESLA DC 90-120kW
Chevy Spark EV	23	400	132 <i>EPA</i>	7 <i>3.3kW</i>	7 <i>3.3kW</i>	---	---	45 min <i>100%</i>	---
Fiat 500e	24	364	140 <i>EPA</i>	6.5	3.5 <i>6.6kW</i>	---	---	---	---
Ford Focus EV	23	318	160 <i>NEDC</i>	6.5	3.5 <i>6.6kW</i>	---	---	---	---
Kia Soul EV	27	375	212 <i>NEDC</i>	7.5	4 <i>6.6kW</i>	---	33 min <i>80%</i>	---	---
Mitsubishi-i-MiEV	16	325	160 <i>NEDC</i>	5 <i>3.3kW</i>	5 <i>3.3kW</i>	---	20 min <i>80%</i>	---	---
Nissan LEAF	24	360	100 <i>NEDC</i>	6.5	3.5 <i>6.6kW</i>	---	30 min <i>80%</i>	---	---
Renault Zoe	22	400	210 <i>NEDC</i>	7 ÷ 9	3	0.5 <i>80%</i>	---	---	---
Smart Electric	17.6	344	109 <i>EPA</i>	5.5 <i>3.3kW</i>	5.5 <i>3.3kW</i>	1 <i>22kW</i>	---	---	---
Tesla S 60	60	---	408 <i>NEDC</i>	16.5	8	---	---	---	30 min <i>80%</i>
Toyota Rav4 EV	41.8	386	166 <i>EPA</i>	11.5	5.5	---	45 min <i>80%</i>	---	---

**Table 1.** Main battery and charging parameters and travel range of some of the most common EVs [5].

common car chargers implement 50kW power and nominal values of 500V and 125A. CAN communication between the car and the charger is used to control the charging process.

- **Tesla Supercharger** – another slight modification of the IEC 62196 Type 2 connector for the European market. This DC standard enables EV charging with up to 120kW at 480V [10] but is supported only by Tesla cars.

From the presented overview of the most common fast DC charging standards, it can be seen that most of them consider similar output power. Thus, a single converter can be implemented in a charging station providing more than one charging standard. Therefore, many EV chargers nowadays support more than one standard for fast charging [11, 12].

### MODULAR SYSTEM APPROACH

When higher output power is required, a proper solution is the use of complex converter systems based on modular principle. Four different modular topologies may be realized with respect to the connections to the load and to the power supply (either in series or in parallel), each of them providing different benefits:

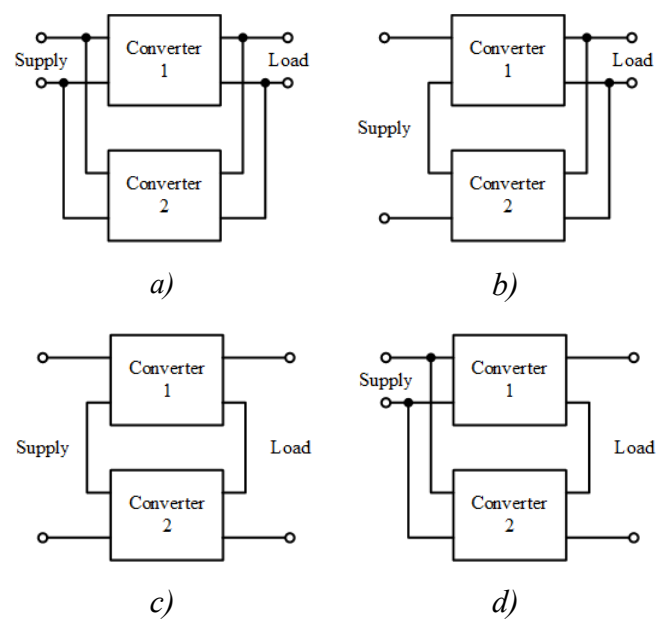
- **IPOP** – input-parallel-output-parallel
- **ISOP** – input-series-output-parallel
- **ISOS** – input-series-output-series
- **IPOS** – input-parallel-output-series

Fig. 3 presents visualization of these four modular topologies. A detailed overview of such connections is provided in [13] for DC-DC converters. They can be implemented in different applications [14, 15].

The four topologies are also possible for any other types of converters and converter modules with the frequencies and the phases of the AC sides taken into consideration. They can be implemented for realization of either the whole converter system or only a specific part of it. Moreover, any combination of them can be used within a single converter system.

### DC BUS REALIZATION

According to the presented in Table 1 battery parameters and the considered



**Fig. 3.** Possible modular connections with respect to the load and to the power supply: a) IPOP; b) ISOP; c) ISOS; d) IPOS.

standards, a converter for fast charging must be able to operate at output voltage up to 500V and output power up to several tens of kW. Thus, the circuit must also withstand operation at significantly large charging currents (up to and even over 100A).

In order to provide such output parameters and to optimize the overall converter operation, a modular approach is proposed for the realization of its output DC Bus. The topology consists of several identical modules connected to the load either in series (providing higher output voltage) or in parallel (providing higher output current). As the maximum output voltage is not expected to exceed the common power devices maximum allowable values, a parallel connection to the load is more appropriate. Nevertheless, both the connections are investigated in the paper. The power supply connection is not considered as it depends mainly on the source of supply.

Fig. 4 presents the proposed converter topologies. It can be observed that current sources are used to supply the load, which is very convenient for realization of a constant-current charging process. This is the most common operating mode used for charging up to at least 80% of the overall battery capacity.

The current sources have a sinusoidal output and are realized on the base of resonant inverters with soft switching. A suitable circuit [16] of such converter is presented in fig. 5.

The proposed topology implements a high-frequency transformer for galvanic isolation.

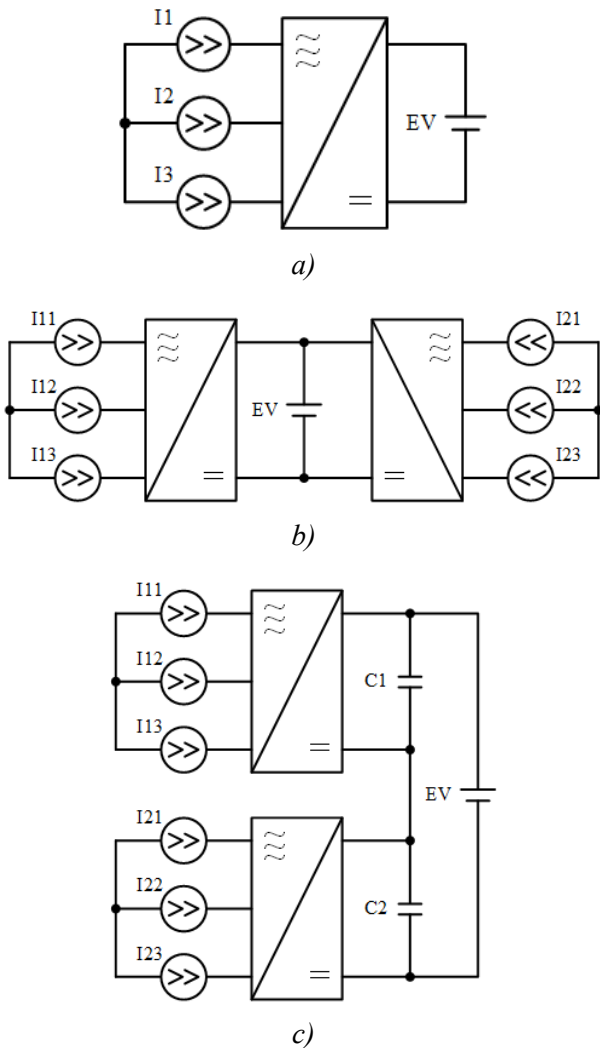


**Fig. 4.** Examined converter topologies: a) basic converter module; b) parallel load connection; c) series load connection.

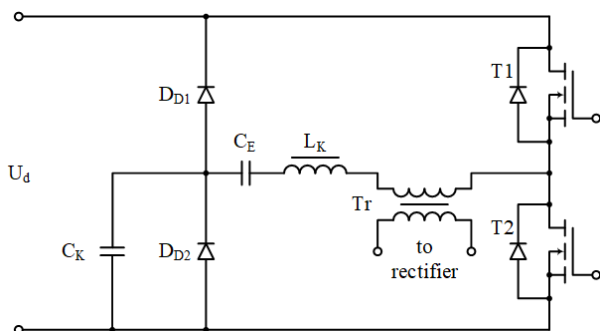


**Fig. 5.** Circuit of a soft switching resonant inverter proposed for realization of the current sources.

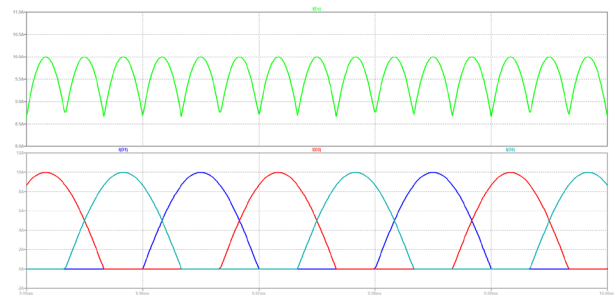
A specificity in the series load connection topology is the use of output filter capacitors as current sources are not suitable for direct series connection. The filter capacitors

transform the outputs into voltage sources providing the opportunity for direct series connection.

## SIMULATION RESULTS

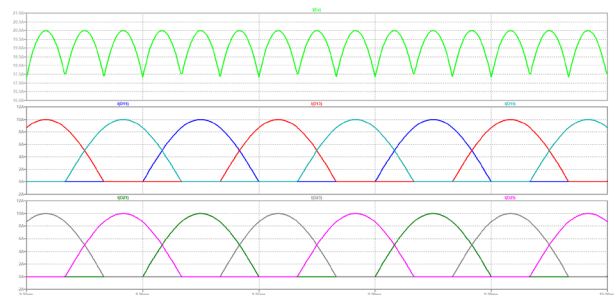
In order to examine the behavior of the presented in fig. 4 proposed converter topologies, computer simulations are carried out. For this purpose, models of the investigated circuits are developed in the software environment of LTspice. Three-phase bridge topology is used for realization of the rectifiers.

Fig. 6 presents waveforms of the basic module output and rectifier diode currents. A specificity in the rectifier operation is the simultaneous conduction of two diodes from one and the same group (anode or cathode) during parts of the half wave period.



**Fig. 6.** Waveforms of output and rectifier currents (basic converter module).

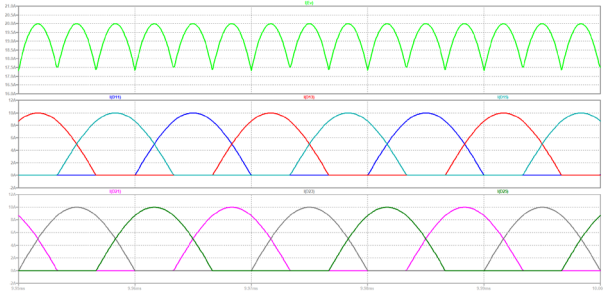
Fig. 7 presents waveforms of the parallel load connection output and rectifier diode currents. Similar waveforms can be obtained for different phase shifts between the current sources of the two converter modules. Fig. 8 presents waveforms obtained for a 60-degree phase shift.



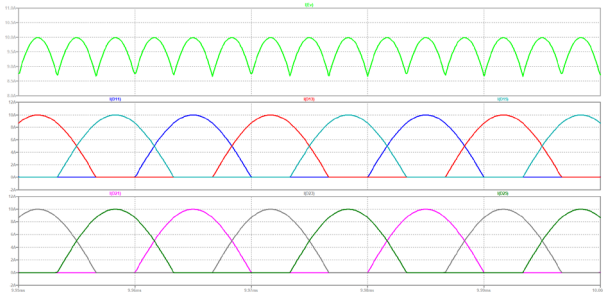
**Fig. 7.** Waveforms of output and rectifier currents (parallel load connection).

Fig. 9 presents waveforms of the series load connection output and rectifier diode currents.

Analogically, similar waveforms can be obtained for different phase shifts between the current sources of the two converter modules. Fig. 10 presents waveforms obtained for a 60-degree phase shift.



**Fig. 8.** Waveforms of output and rectifier currents (parallel load connection, 60-degree phase shift).



**Fig. 9.** Waveforms of output and rectifier currents (series load connection).

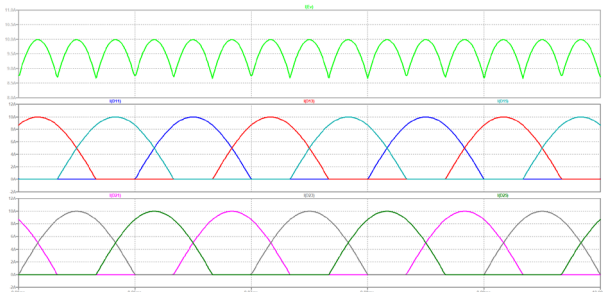


**Fig. 10.** Waveforms of output and rectifier currents (series load connection, 60-degree phase shift).

Equation (1) presents the basic module (fig. 4a) average output current value of as function of the maximum current source values:

$$I_{EV,AVE} = \frac{3}{\pi} \int_{\frac{\pi}{6}}^{\frac{\pi}{6}} I_{MAX} \cos \Theta d\Theta = \frac{3}{\pi} I_{MAX} \quad (1)$$

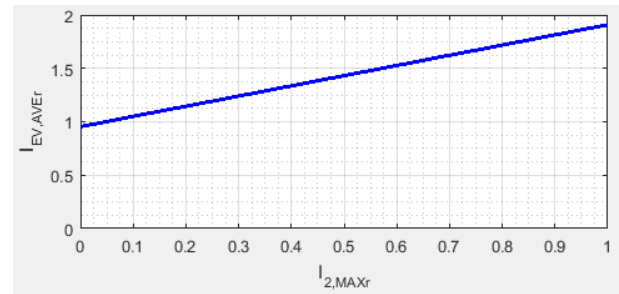
where  $I_{EV,AVE}$  is the average value of the rectified output current and  $I_{MAX}$  is the maximum value of the sinusoidal source currents.

When two converter modules operate in parallel to the load (fig. 4b), the average output current value is obtained according to equation (2):

$$I_{EV,AVE} = I_{EV1,AVE} + I_{EV2,AVE} = \frac{3}{\pi} (I_{1,MAX} + I_{2,MAX}) \quad (2)$$

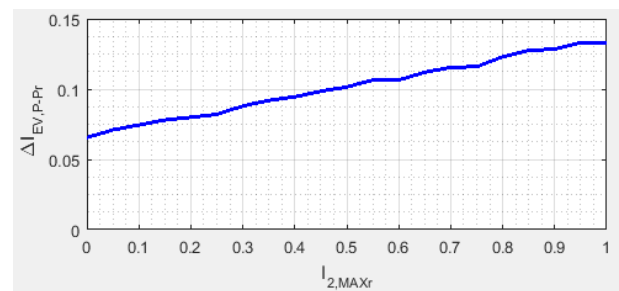
where  $I_{1,MAX}$  and  $I_{2,MAX}$  are the maximum values of the two converters input current sources. Varying one or both of these two values, different charging currents can be obtained.

Fig. 11 presents the average output current  $I_{EV,AVEr}$  as function of the maximum current source value  $I_{2,MAXr}$ . Both currents are normalized to the nominal maximum input current value  $I_{2,MAX}$ .



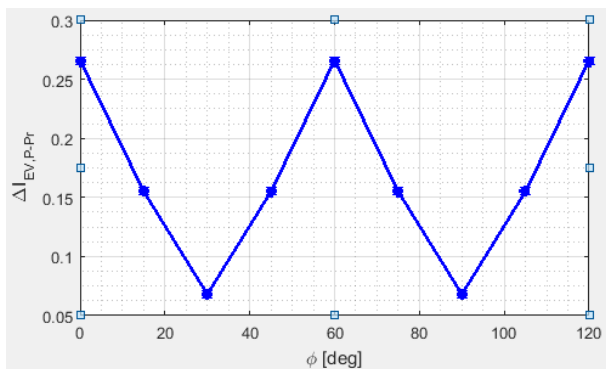
**Fig. 11.** Average output current as function of the maximum input current  $I_{2,MAX}$ .

Fig. 12 presents the peak-to-peak output current ripple  $\Delta I_{EV,P-Pr}$  as function of the maximum current source value  $I_{2,MAXr}$ . Both currents are normalized to the nominal maximum input current value  $I_{2,MAX}$ .



**Fig. 12.** Output current ripple (peak to peak) as function of the maximum input current  $I_{2,MAX}$ .

Fig. 13 presents the peak-to-peak output current ripple  $\Delta I_{EV,P-Pr}$  as function of the phase shift  $\varphi$  between the sources of the two converter modules. The current is normalized to the nominal maximum input current value  $I_{2,MAX}$ .



**Fig. 13.** Output current ripple (peak to peak) as function of the phase shift.

## CONCLUSION

For realization of a fast DC charging station, parallel load connection is suitable. The connected in parallel modules consist of high-frequency current sources and three-phase rectifiers. The parallel load connection allows control of the charging current by variation of one or both converters current source values.

With variation of one of the converters current source values, the output current peak-to-peak ripple varies. It also depends on the phase shift between the sources of the two converter modules, having minimum values at phase-shift angles of 30 and 90 degrees.

Different types of resonant inverters can be used for current sources in the proposed topologies. As the maximum current value of these converters significantly depends on the load impedance and the resonant tank quality factor, it is recommended resonant inverters with improved output characteristics such as the proposed one (fig. 5) to be used.

## ACKNOWLEDGEMENTS

The carried out research is realized in the frames of the project "Model based design of power electronic devices with guaranteed parameters", ДН07/06/15.12.2016, Bulgarian National Scientific Fund.

## REFERENCES

- [1] Shanan, Z., *Tesla Model S & Nissan LEAF Clocked As World's Best-Selling Electric Cars In 2016*, Clean Technica, Feb. 4, 2017, [cleantechnica.com](http://cleantechnica.com).
- [2] Randall, T., *Here's How Electric Cars Will Cause the Next Oil Crisis*, Bloomberg, Feb. 25, 2016, [bloomberg.com](http://bloomberg.com).
- [3] Yoshio, M., A. Kozawa, R. J. Brodd, *Lithium-ion batteries. Science and technologies*, Springer, 2013.
- [4] Hannan, M. A., M. S. H. Lipu, A. Hussain, A. Mohamed, *A review of lithium-ion battery state of charge estimation and management system in electric vehicle applications: Challenges and recommendations*, Renewable and Sustainable Energy Reviews, vol. 78, Oct. 2017, pp. 834-854.
- [5] Guinn, S., *Level 1 vs Level 2 EV charging*, ClipperCreek, Feb. 9, 2017, [clippercreek.com](http://clippercreek.com).
- [6] Type 2 connector – [https://en.wikipedia.org/wiki/Type\\_2\\_connector](https://en.wikipedia.org/wiki/Type_2_connector).
- [7] Combined Charging System – [https://en.wikipedia.org/wiki/Combined\\_Charging\\_System](https://en.wikipedia.org/wiki/Combined_Charging_System).
- [8] CHAdeMO – <https://en.wikipedia.org/wiki/CHAdeMO>.
- [9] CHAdeMO, *Technology Overview* – <http://www.chademo.com/technology/technology-overview/>.
- [10] Tesla Supercharger – [https://en.wikipedia.org/wiki/Tesla\\_Supercharger](https://en.wikipedia.org/wiki/Tesla_Supercharger).
- [11] ABB, *Terra 53 multi-standard DC charging station*, Product Leaflet, 2016.
- [12] Schneider Electric, *EVlink DC Level 3 Networked Pedestal 50kW Dual Vehicle Fast Charging Station*, EVDC48050CHACCS Product Datasheet, Oct. 10, 2017.
- [13] Chub, A., O. Husev, D. Vinnikov, *Input-Parallel Output-Series Connection of Isolated Quasi-Z-Source DC-DC Converters*, Electric Power Quality and Supply Reliability Conference (PQ), June 11-13, 2014, pp. 277-284.
- [14] Park, K., Z. Chen, *Analysis and Design of a Parallel-Connected Single Active Bridge DC-DC Converter for High-Power Wind Farm Applications*, 15<sup>th</sup> European Conference on Power Electronics and Applications (EPE), Sept. 2-6, 2013.
- [15] Hayashi, Y., M. Mino, *Series-Parallel Connected 10W/cm<sup>3</sup> DC-DC Converter for Advanced High-Density Converter Design*, 33<sup>rd</sup> IEEE International Telecommunications Energy Conference (INTELEC), Oct. 9-13, 2011.
- [16] Vuchev, S., D. Arnaudov, N. Hinov, *Comparative Analysis of Resonant Converters for Energy Storage Systems*, 21<sup>st</sup> International Conference on Circuits, Systems, Communications and Computers, July 14-17, 2017.